Title	FEM Simulation of the Spot Welding Process (Report II) : Effect of Initial Gap and Electrode-type on Nugget Formation and Expulsion(Mechanics, Strength & Structure Design)
Author(s)	Zhang, Jianxun; Murakawa, Hidekazu
Citation	Transactions of JWRI. 1998, 27(2), p. 73-79
Version Type	VoR
URL	https://doi.org/10.18910/8463
rights	
Note	

FEM Simulation of the Spot Welding Process (Report II)†

- Effect of Initial Gap and Electrode-type on Nugget Formation and Expulsion -

Jianxun ZHANG* and Hidekazu MURAKAWA**

Abstract

A procedure is developed to estimate expulsion occurrence in spot welding based on the theoretical analysis and FEM. The expulsion will occur when the nugget radius is larger than the contact radius between plate to plate. The nugget formation and expulsion occurrence of a high tensile carbon steel were analyzed for spot welding with initial gap and three type electrodes, Dome-type, R-type(40mm) and R-type(100mm). Conclusions show that the nugget formation is greatly affected by initial gap and electrode type. The initial gap affects not only the static contact but also the kinetic contact. The initial formation of the nugget is advanced by the initial gap for the Dome-type electrode and R-type(40mm) electrode. However, the initial formation of the nugget is delayed by the initial gap for the R-type(100mm) electrode when the initial gap exceeds 2.0mm. The effect of the initial gap on the nugget radius at 12 welding cycles is small for Dome-type and R-type (40mm), but large for R-type (100mm) electrodes. The expulsion occurrence is affected by initial gap and electrode type. The expulsion occurrence increases with an increase of initial gap. The expulsion occurrence of the R-type(100) electrode is less than that of the R-type(40mm) and Dome-type electrode. The expulsion occurrence is almost the same between Dome-type and R-type(40mm) electrodes.

KEY WORDS: (Spot Welding) (Expulsion) (Initial Gap) (Finite Element Method)

1. Introduction

The load-bearing capacity of the weldment in spot welding is dependent on the nugget dimensions such as nugget diameter and thickness. The larger the nugget size, the better the load-bearing capacity of the weldment. The proper expulsion in the operation of spot welding process is desirable to achieve the largest nugget size. However, larger expulsion in spot welding will impair the labour condition and the quality of weldment. The occurrence of expulsion is affected by many factors such as welding current, squeezing force, welding time and so on. How and when the expulsion will happen is very important but a difficult problem in order to keep good and stable quality of weldment in the spot welding process. Much attention has been paid to improving the quality of weldments in spot welding[1-5].

There always exists a gap, called an initial gap, in the thin plates to be welded by spot welding. Based on experiments on the effect of initial gap on nugget formation, it has been reported that the weldability is strongly influenced by the contact states of both electrode to plate and plate to plate, and appropriate welding conditions to improve the weldability were proposed[6]. Numerical analyses of deformation under squeezing processes in spot welding with a gap were made using a finite element method[7]. On the basis of the numerical analysis, the squeezing process can be divided into three stages with respect to plastic deformation and large deformation. Further, to predict the electrode force required to close the initial gap, two methods, using parametric curves and approximation curves respectively, have been proposed. The effect of initial gap on nugget formation and contact state was examined numerically using a self-developed thermal elastic-plastic finite element code with small deformation theory[8]. The spring element was used to deal with the contact problem between electrode to plate and plate to plate. The results show that the initial gap has a large effect on the contact states between plate to plate and electrode to plate.

In this report, a finite element code is perfected as an incremental coupled thermal elastic-plastic large

† Received on December 4, 1998
* Foreign Research Fellow,
(Professor, Xi'an Jiaotong University)
** Associate Professor

Transactions of JWRI is published by Joining and Welding Research Institute of Osaka University, Ibaraki, Osaka 567-0047, Japan.

deformation problem to simulate the spot welding process. An approach is introduced to estimate the expulsion occurrence in spot welding. The nugget formation and expulsion possibility of a high-tensile carbon steel were analyzed for spot welding with initial gap for three type electrode, Dome-type, R-type(40mm) and R-type(100mm).

2. Governing equations

2.1 Static electric field:

The governing equation for a static electric field in spot welding can be treated as an axisymmetric problem.

$$\frac{1}{r}\frac{\partial}{\partial r}\left(r\varepsilon\frac{\partial\phi}{\partial r}\right)+\frac{\partial}{\partial z}\left(\varepsilon\frac{\partial\phi}{\partial z}\right)=0 \tag{1}$$

where, r and z are radial and axial coordinates, ε is the electric conductivity, φ is the electric potential.

There are two types of boundary condition for spot welding shown as follows:

On the boundary facing air:

$$\frac{\partial\phi}{\partial n}=0 \tag{2}$$

On the surface of electrode:

$$\int_S \varepsilon\frac{\partial\phi}{\partial n}ds = I\sin(\omega t) \tag{3}$$

where, $\partial\phi/\partial n$ is the gradient along the outward normal direction of the boundary and the integral is taken on the cross section of the electrode.

2.2 Heat conduction

The unsteady state heat conduction with internal heat generation in the axisymmetric form can be expressed by:

$$c\rho\frac{\partial T}{\partial t}=\frac{1}{r}\left\{\frac{\partial}{\partial r}\left(\lambda r\frac{\partial T}{\partial r}\right)+\frac{\partial}{\partial z}\left(\lambda r\frac{\partial T}{\partial z}\right)\right\}+Q \tag{4}$$

where, T is temperature (°C), C the heat capacity, r the density, λ heat conductivity, Q is the rate of internal heat generation per unit volume.

There are three kinds of boundary condition for heat conduction in spot welding.

$$T=T_B \quad \text{given temperature} \tag{5}$$

$$-\lambda\frac{\partial T}{\partial n}=\alpha(T-T_0) \quad \text{given heat transfer} \tag{6}$$

$$-\lambda\frac{\partial T}{\partial n}=q_B \quad \text{given heat flux} \tag{7}$$

The internal heat generation rate, Q can be expressed by the following:

$$Q=\frac{1}{\varepsilon}J^2 \tag{8}$$

where, J is current density.

2.3 Thermal elastic plastic large deformation analysis

The relationship between the strain and displacement for large deformation in axisymmetric conditions is given by[9]:

$$\varepsilon_r=\frac{\partial u_r}{\partial r}+\frac{1}{2}\left\{\left(\frac{\partial u_r}{\partial r}\right)^2+\left(\frac{\partial u_z}{\partial r}\right)^2\right\} \tag{9}$$

$$\varepsilon_z=\frac{\partial u_z}{\partial z}+\frac{1}{2}\left\{\left(\frac{\partial u_r}{\partial z}\right)^2+\left(\frac{\partial u_z}{\partial z}\right)^2\right\} \tag{10}$$

$$\varepsilon_\theta=\frac{u_r}{r}+\frac{1}{2}\left(\frac{u_r}{r}\right)^2 \tag{11}$$

$$\varepsilon_{rz}=\frac{1}{2}\left(\frac{\partial u_r}{\partial z}+\frac{\partial u_z}{\partial r}\right)+\frac{1}{2}\left\{\frac{\partial u_r}{\partial z}\frac{\partial u_r}{\partial r}+\frac{\partial u_z}{\partial r}\frac{\partial u_z}{\partial z}\right\} \tag{12}$$

where, ε_r, ε_z, ε_θ and ε_{rz} are strain components, and u_r and u_z are displacements in the radial and axial directions.

Since the thermal elastic plastic large deformation behavior in spot welding is a highly nonlinear phenomenon, the stress-stain relation is described by incremental matrix forms.

$$\{d\varepsilon\}=[B]\{d\delta\} \tag{13}$$

where, $[B]=[B_0]+[B_L(\{\delta\})]$, $[B_0]$ is the ordinary strain matrix in small deformation theory, $[B_L(\{\delta\})]$ is the large deformation strain matrix related to the present displacement $\{\delta\}$.

The stress increment with the thermal strain can be expressed by[10]:

$$\{d\sigma\}=[D_{ep}]\{d\varepsilon\}-[C]dT \tag{14}$$

where, $[D_{ep}]$ is the elastic-plastic strain-stress matrix, $[C]$ the temperature-stress transfer matrix.

The equilibrium equation can be described as the following virtual work theorem form in incremental form.

$$\int_V(ds_{ij}\,\delta\varepsilon_{ji})dV+\int_V s_{ij}dB_{ji}\delta u_i dV=\int_S(dF_{ni}\delta u_i)dS \tag{15}$$

where, $\delta\varepsilon_{ji}$ and δu_i are virtual strain and displacement, s_{ij} the nominal stress, F the boundary force in the boundary S.

In the equilibrium state:

$$s_{ij}=\sigma_{ij} \tag{16}$$

$$F_{ni}=s_{ji}n_j \tag{17}$$

In the deformation state, the effect of rotation strain on the stress state should be taken into account[11].

$$ds_{ij}=d\sigma_{ij}+\sigma_{ik}\frac{\partial du_j}{\partial x_k}-\sigma_{ik}d\varepsilon_{kj}-\sigma_{jk}d\varepsilon_{ki} \tag{18}$$

According to the above relations, the finite element matrix can be formed as follows.

$$[dK]\{du\}=\{dF\} \tag{19}$$

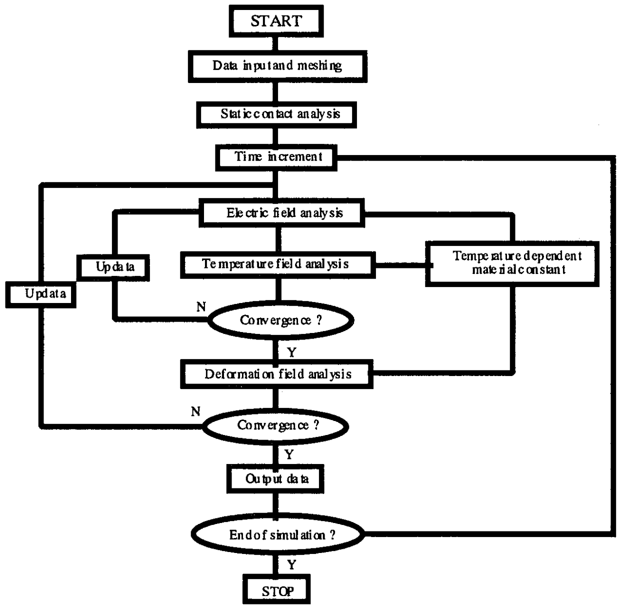

Fig.1 scheme for spot welding analysis.

where, $[dK]=[dK_e]+[dK_L]+[dK_\sigma]+[dK_\omega]$. The matrix $[dK_e]$ is the ordinary stiffness matrix in the small deformation theory, $[dK_L]$ the large deformation matrix according to the strain matrix in equation(13), $[dK_\sigma]$ the large deformation form related to the present stress, $[dK_\omega]$ the effective matrix because of the rotation strain in the large deformation state, $\{dF\}$ the load vector according to the external force and thermal loading. The matrix can be expressed as following:

$$[dK_e]=\int_V[B_0]^T[D_{ep}][B_0]dV \tag{20}$$

$$[dK_L]=\int_V[B_0]^T[D_{ep}][B_L]dV+\int_V[B_L]^T[D_{ep}][B_L]dV+\int_V[B_L]^T[D_{ep}][B_0]dV \tag{21}$$

$$[dK_\sigma]=\int_V d[B]^T\{\sigma\}dV \tag{22}$$

$$[dK_\omega]=\int_V[N_k]_{,i}{}^T\sigma_{ij}[N_k]_{,j}dV-\int_V[B_{ki}]^T\sigma_{ij}[B_{kj}]dV \tag{23}$$

$$\{dF\}=\int_S[N]^T\{dp\}dS+\int_V[B]^T[D_{ep}][c]dTdV \tag{24}$$

Based on the equations mentioned above, a finite element code was formed. For the spot welding process with an initial gap, there are three coupled problems: electric field problem, heat conduction problem and thermal elastic-plastic large deformation problem. To solve this type of coupled problem in a strict manner, simultaneous solutions of the electric, the thermal and the mechanical fields are necessary. However, due to the complexity and the cost of the analysis, an alternative approximate method is employed in the present program. Instead of solving the three fields simultaneously, the three field analysis is coupled to each other for every time increment. The scheme used in computation is shown in the **Fig.1.**

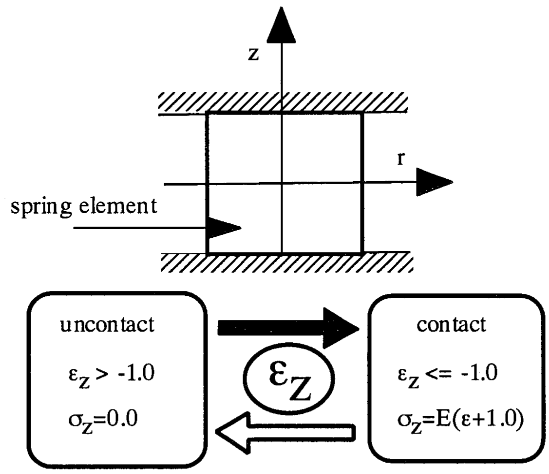

Fig.2 The conditions of contact states

A spring-type surface element is introduced to simulate the contact stages of the interfaces between electrode to plate and plate to plate. The condition for judgment of contact or no-contact is shown in **Fig.2.** When the reaction force acting on the spring is compressive, the corresponding part of the interface is judged to be in contact. If the interface is in contact, the stiffness of the spring is set large enough to be considered as a rigid link. When the reaction force becomes tensile, there is judged to be no-contact and the stiffness of the spring is set to be zero to cut the link. The transition from no-contact to contact is judged from the element strain in the z direction.

3. Analysis Model and Procedure

In general, the forms of spot welding joints largely depend on the types of the structures. An axisymmetric configuration is assumed in this paper. The model of the spot welding process with an initial gap is shown in **Fig.3**. Because of the symmetry, only one quarter of the model is analyzed with a mesh of 2016 elements and 2283 nodes of four-node isoparametric elements. The 78 spring elements were included in the mesh between electrode to plate and plate to plate. The Dome-type and R-type electrode are used in the analysis and their shapes near the tip of the electrode are illustrated in **Fig.4**. The tip of the Dome-type electrode is spherical with a radius 40 mm within 3 mm of its center and it is tapered with a radius 8 mm outside the spherical tip. The tip of R-type electrode is spherical with its radii of 40 mm and 100 mm respectively. The initial gap exists and changes from 0.0 mm to 4.0 mm between the plates to be

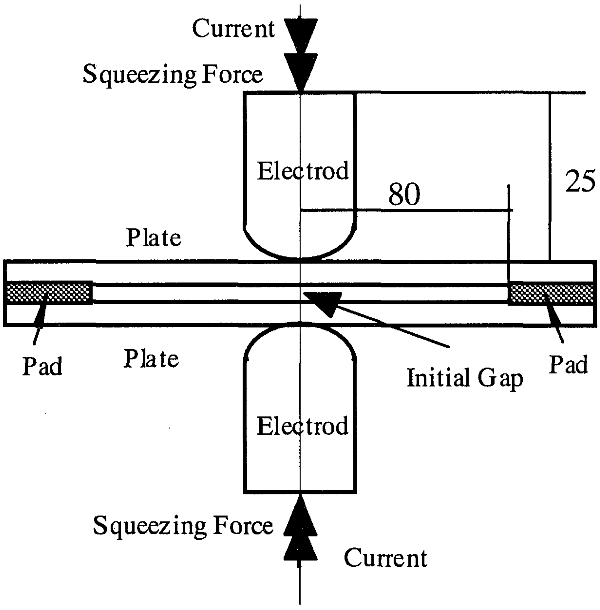

Fig.3 The model of spot welding

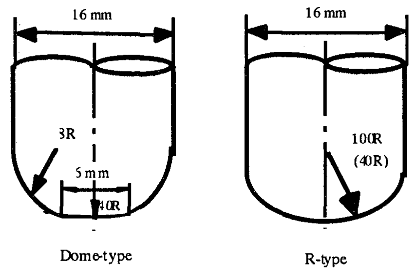

Fig.4 The Dome-type and R-type electrode

welded. The thickness of the plate to be welded is assumed to be 1.2 mm. The material used is a high-tensile carbon steel. The melt temperature is 1480℃. The mechanical properties and thermal constants of the plate to be welded are dependent on temperature[8].

4. Estimation of expulsion occurrence

Large expulsion in spot welding has an effect on the labour condition and load-bearing capacity of the weldment. Physically, expulsion in spot welding allows molten metal to burst out between the plates to be welded under the squeezing force. The occurrence of expulsion is affected by many factors such as welding current, squeezing force, welding time and so on. In general, the expulsion possibility will decrease with the decrease of squeezing force and welding current. To estimate correctly the expulsion occurrence is very important to improve the quality of the weldment in the spot welding process. The illustration of expulsion in spot welding is shown in **Fig.5**. It can be assumed from **Fig.6** that the contact radius and the nugget radius

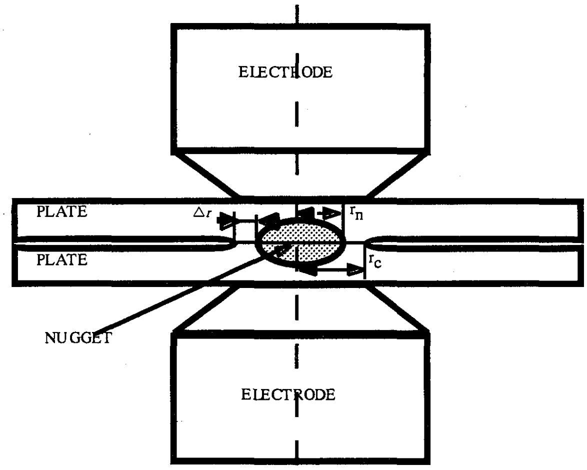

Fig.5 The model for expulsion in spot welding

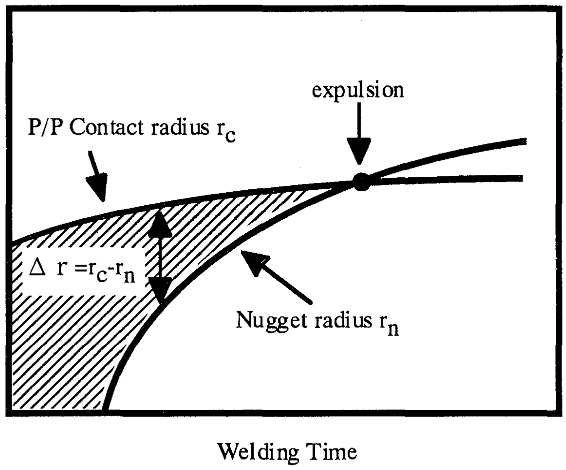

Fig.6 Illustration of expulsion occurrence in spot welding

will increase with the welding time and that a critical point is reached when the nugget radius exceeds the contact radius because of the flow of hot liquids. From this point, an approach to estimate expulsion occurrence in spot welding is introduced based on a calculation of contact radius and nugget radius as follows:

$$\Delta r = r_c - r_n \le 0 \tag{25}$$

where, r_c is the contact radius between electrode and plate, r_c the nugget radius.

The parameters shown in equation(25) can be computed by finite element method.

5. Results and discussion

The development of the nugget diameter with welding time for three types of electrode is illustrated in **Fig.7**. The squeezing force and the initial gap are assumed as 200kgf and 2.0 mm respectively. The welding current is 9000A. It can be seen that the nugget diameters increase with welding time and that the initial formation time of the nugget is dependent on the electrode type. The lines of the nugget development are almost the same for the Dome-type electrode and R-type(40mm) electrode. There are two parameters, the initial formation time of the nugget and the nugget radius at 12 cycle welding time which can be used to describe the characteristics of the nugget development line. The initial formation time of the nugget with initial gap for three types of electrode is shown in **Fig.8**. The squeezing force is 200kgf. The welding current is 9000A. It can be seen from **Fig.8** that the initial formation time of the nugget decreases with an increase of the initial gap for Dome-type electrode and R-type(40mm) type electrode and that there are some large changes for the R-type (100mm) electrode when the initial gap is larger than 2.0mm. The reason for the phenomenon in the R-type (100) electrode is interpreted as meaning that the contact state between electrode to plate has some effect on the formation of the nugget. There exists a ring-like no-contact region in the active contact surface of the electrode as shown in **Fig.9**. The line marked by solid triangles, called line A, shows the contact region from the center of the electrode. The region between line A and Line B marked by solid squares is the so called ring-like no-contact one. The line marked by solid circles denotes the contact region from line B. The contact states change with welding time. It is found from the numerical analysis that the ring-like no-contact region appears when the initial gap exceeds 2 mm for R-type electrode (100mm) and that there is no ring-like no-contact region in the Dome-type and R-type (40mm) electrodes. The contact states between electrode to plate and plate to plate are very complicated problems, which are dependent on constraint, material properties and welding parameters.

The nugget radii after 12 cycles for Dome-type and

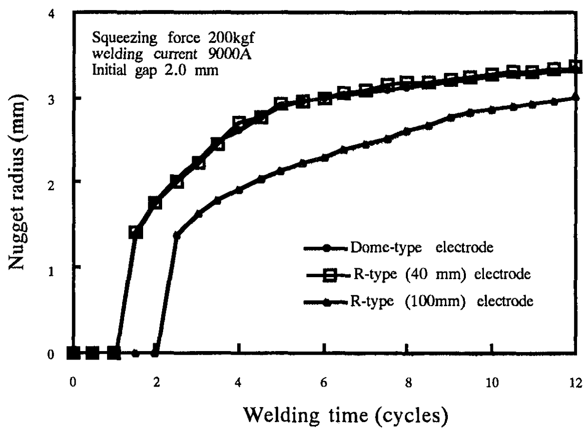

Fig.7 Development of nugget radius with welding time for different electrodes.

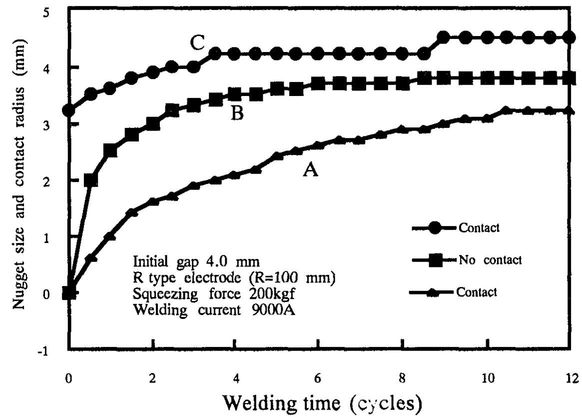

Fig.9 Development of contact states between electrode and plate for the R-type electrode(100mm).

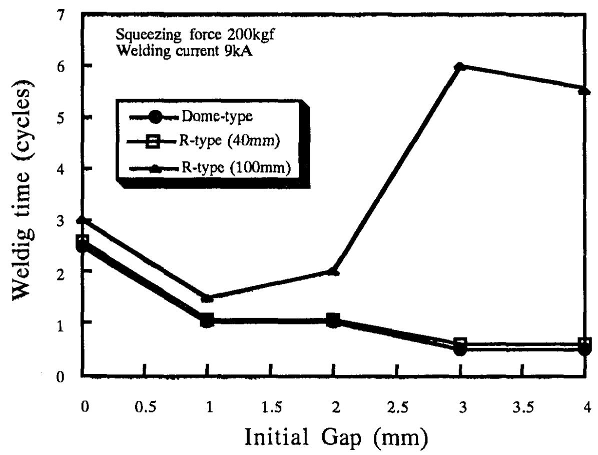

Fig.8 The relationship between initial nugget formation with initial gap for different electrode.

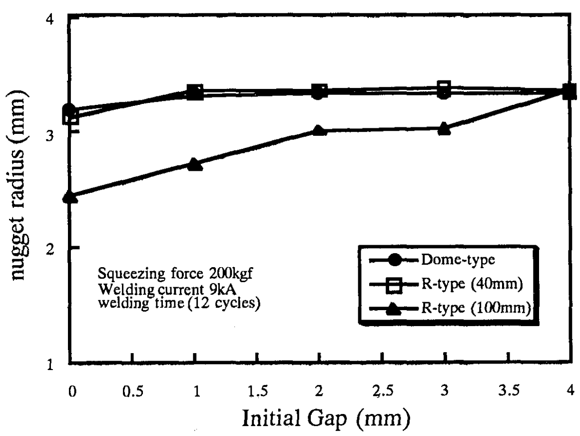

Fig.10 The relationship between nugget radius after 12 welding cycles and initial gap for different electrodes

R-type electrodes are shown in **Fig.10**. The nugget radius increase with the initial gap. The nugget radii are almost the same when the initial gap exceeds 1 mm for Dome-type and R-type(40mm) electrodes. However, the nugget radius is changing with initial gap size for the R-type(100mm) electrode. Therefore, the electrode with a large spherical radius is more sensitive to initial gap. It is better to use the Dome-type and R-type electrodes with spherical radii less than 40 mm in order to achieve a stable nugget size.

The expulsion occurrence in spot welding can be estimated by comparing the nugget radius with contact radius between plate to plate. One example is shown in **Fig.11** for an R-type(40mm) electrode with 2.0mm initial gap. The squeezing force and welding current are 200kgf and 9000A respectively. It can be seen that the nugget radius and contact radius between plate to plate increase with an increase of welding time and that the expulsion would happen at about 5 welding cycles.

Another example is shown in **Fig.12** for a Dome-type electrode with a 1.0mm initial gap. The squeezing force and welding current are 200kgf and 8000A respectively. There is no intersection between nugget radius and contact radius in **Fig.12**. This means that the expulsion would not occur in this welding condition.

The relationships between expulsion occurrence time and initial gap are shown in **Fig.13** for Dome-type electrode with different welding currents. The squeezing force is assumed as 200 kgf. It can be seen that the expulsion possibility increases with initial gap size and that the larger the welding current is, the larger the expulsion possibility becomes. The difference of expulsion possibility among three types of electrode is expressed in **Fig.14**. The squeezing force and welding current are assumed 200kgf and 10000A respectively. It can be seen that the expulsion possibility is almost the same between Dome-type and R-type(40mm) electrodes and that the expulsion possibility of an R-type electrode (100mm) is less than that of an R-type electrode (40mm).

6. Conclusion

The nugget formation and expulsion possibility of mild steel in spot welding with initial gap for Dome-type and R-type electrode were analyzed using a finite element program. The conclusions are as follows.

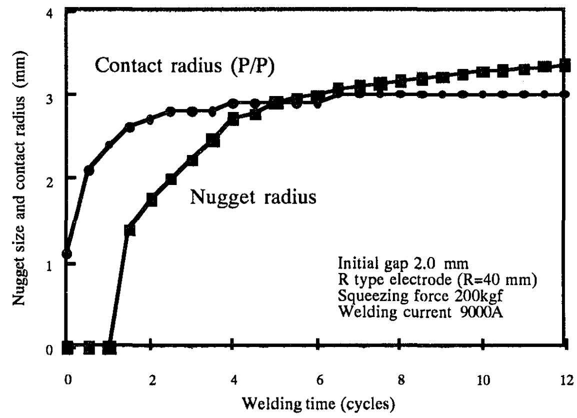

Fig.11 Development of nugget radius and contact radius with welding time for R-type electrode(40mm).

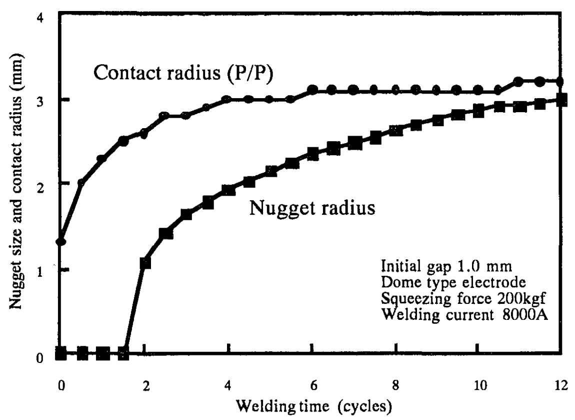

Fig.12 Development of nugget radius and contact radius with welding time for Dome-type electrode.

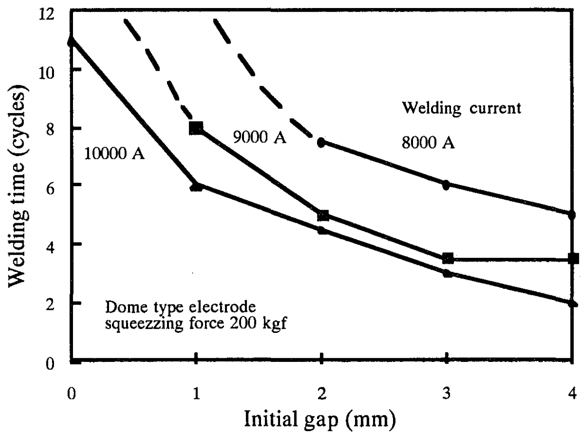

Fig.13 The effect on initial gap and welding current on the expulsion occurrence for Dome-type electrode.

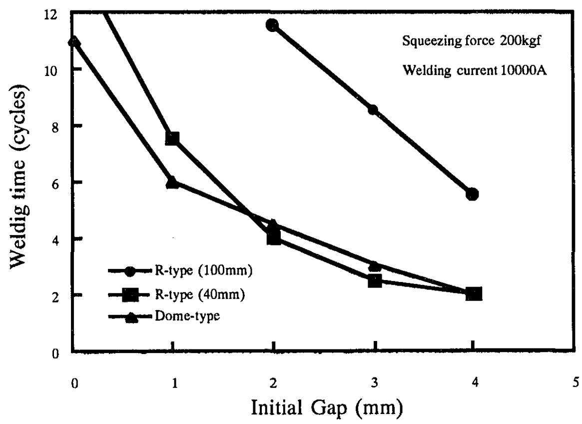

Fig.14 The expulsion occurrence time with initial gap for different electrodes.

The nugget formation and development are greatly affected by initial gap and electrode type. The initial formation of the nugget is advanced by the initial gap for the Dome-type electrode and R-type(40mm) electrode. However, the initial formation of the nugget is delayed by the initial gap for the R-type(100mm) electrode when the initial gap exceeds 2.0mm.

The expulsion occurrence in spot welding can be estimated by comparing the nugget radius with contact radius between plate to plate. The expulsion possibility is affected by the initial gap and the electrode type. The expulsion possibility increases with an increase of initial gap. The expulsion possibility for an R-type(100) electrode is less than for an R-type(40mm) and a Dome-type electrode. The expulsion possibility is almost the same between Dome-type and R-type(40mm) electrodes.

References

1) W.Rice, and E.J.Funk, "Analytical investigation of the temperature distribution during resistance welding", Welding Journal, Vol.46, No.4, 1967, pp175s-182s
2) C.L. Tsai, W.L. Dai, D.W. Dickinson and J.C. Papritan, "Analysis and Development of a Real-Time Control Methodology in Resistance Spot Welding", Welding Research Supplement Dec. 1991, pp339-351.
3) J.M.Sawhill, and J.C.Baker, "Spot weldability of high-strength sheet steels", Welding Journal, Vol.59, No.1, 1980, pp19s-30s
4) H. Murakawa, H. Kimura, and Y. Ueda, "Weldability Analysis of Spot Welding on Aluminum Using FEM", Trans. JWRI, Vol.24, No.1, 1995, pp101-11
5) J.E.Gould, "An Examiniation of Nugget Development during Spot Welding, Using Both Experimental and Analytical Techniques", Welding Journal, 66(1): pp1s-10s.
6) K.Nishiguchi, K.Matruyama and T.Myouga, "Fundamental Study on Spot Welding of Pressformed Mmbers - influences of initial gap and yielding strength of materials - ", Japan Welding Society, Technical Commission on Resistance Welding, Report RW-199-81, 1981, (in Japanese)
7) H.Murakawa and Y.Ueda, "Mechanical Study on the Effect of the Initial Gap upon the Weldability of Spot Weld Joint", Trans. JWRI, Vol.18, No.1, 1989, pp51-58
8) H.Murakawa and J.X.Zhang, "FEM Simulation of Spot Welding Process (Report I), --Effect of Initial Gap on Nugget formation --", Trans. JWRI, Vol.27(1998), No.1, pp75-82.
9) A.J.Durelli, E.A.Pehillips, C.H.Tsao, "Introduction to the Theoretical and Experimental Analysis of Stress and Strain", McGRAW-HILL Book Company, INC, 1958
10) Y.Ueda, and T.Yamakawa, "Analysis of Thermal Elastic-Plastic Stress and Strain During Welding by Finite Element Method", Trans of JWS, Vol.2, No.2, 1971.pp90-100.
11) Manabu GoToh, "Engineering Finite Element Method--For Analysis of Large Elastic-Plastic Deformation", Corona Publishing Co. Ltd., 1995.